

Full-length Research Paper (Toxicology)

**A toxicoproteomic study on cardioprotective effects of pre-administration of docetaxel in
a mouse model of adriamycin-induced cardiotoxicity**

Kaname Ohyama^{a,b*}, Mari Tomonari^c, Tomoko Ichibangase^d, Hideto To^c, Naoya Kishikawa^a,
Kenichiro Nakashima^e, Kazuhiro Imai^d, and Naotaka Kuroda^a

^aDepartment of Environmental and Pharmaceutical Sciences, Graduate School of Biomedical Sciences,
Nagasaki University, Nagasaki, Japan

^bNagasaki University Strategy for Fostering Young Scientists, Nagasaki, Japan

^cDepartment of Hospital Pharmacy, Nagasaki University Hospital, Nagasaki, Japan

^dResearch Institute of Pharmaceutical Sciences, Musashino University, Nishitokyo-shi, Tokyo, Japan

^eDepartment of Clinical Pharmacy, Graduate School of Biomedical Sciences, Nagasaki University,
Nagasaki, Japan

*Corresponding author. Department of Environmental and Pharmaceutical Sciences, Graduate School
of Biomedical Sciences, Nagasaki University, 1-14 Bunkyo-machi, Nagasaki 852-8521, Japan.

Tel/Fax: +81-95-819-2446; E-mail: k-ohyama@nagasaki-u.ac.jp

Abstract

Studies suggest that pre-administration of docetaxel (DOC) in a doxorubicin (ADR)-DOC combination anticancer therapy results in stronger antitumor effects and fewer ADR-induced cardiotoxic deaths in mouse model, yet no mechanism explaining this effect has been established. The aim of this study was to identify cellular processes in mouse heart tissue affected by different ADR/DOC dosing protocols using a toxicoproteomic approach. We applied fluorogenic-derivatization liquid chromatography tandem mass spectrometry (FD-LC-MS/MS) - which consists of fluorogenic derivatization, separation and fluorescence detection by LC, and identification by LC-tandem mass spectrometry - to the proteomic analysis of heart tissue from control, intermittent-dosing (DOC-ADR), and simultaneous-dosing (ADR&DOC) groups. In DOC-ADR group, ADR was administered 12 h after DOC injection; in ADR&DOC group, both drugs were administered simultaneously; in control group, saline was administered at the same timing as ADR injection of other groups. Heart samples were isolated from all mice 1 week after the treatment. The highly reproducible and sensitive method (FD-LC-MS/MS) identified nine proteins that were differentially expressed in heart tissue of control and the two treatment groups; seven of these nine proteins participate in cellular energy production pathways, including glycolysis, the tricarboxylic acid cycle, and the mitochondrial electron transport chain. Significantly higher expression of glyceraldehyde-3-phosphate dehydrogenase (GAPDH) was observed in the DOC-ADR group, the group with the fewer cardiotoxic deaths, than in the ADR&DOC group. Therefore, GAPDH may have potential as a drug target for protective intervention and a biomarker for

evaluation of the cardioprotective effects in pre-clinical studies.

Keywords: doxorubicin-induced cardiotoxicity; docetaxel re-administration; fluorogenic derivatization-liquid chromatography tandem mass spectrometry; toxicoproteomics

1. Introduction

Although adriamycin (ADR) is an anthracycline anticancer drug that has been widely applied in treating a range of cancers (e.g., lymphoma, leukemia, breast cancer, and ovarian cancer), severe cardiotoxicity and heart failure have been observed in ADR-treated cancer patients [1]. In clinical trials for metastatic breast cancer, an ADR and docetaxel (DOC) combination therapy is much more effective than the previous combination therapies (*i.e.*, ADR-cyclophosphamide and fluorouracil-ADR-cyclophosphamide) [2, 3]. However, severe toxicities including myelosuppression and cardiotoxicity limit the clinical use of ADR/DOC combination therapy in many patients with breast cancer [2-4].

Many attempts have been made to reduce the adverse effects induced by anticancer drugs, and one such approach has been chronotherapy. Chronotherapy is defined as the administration of medications using biological rhythms to optimize therapeutic outcomes and/or control adverse effect. The chronopharmacology of many antitumor drugs have been studied in human and animals specifically to decrease adverse effects [5-16]. The individual toxicities of ADR and DOC apparently depend on dosing time in animals and human [8-13]. Among the chronopharmacologic studies, To and colleagues reported that the DOC-pretreated group, in which ADR was administered 12 h after DOC injection, exhibited not only stronger inhibition of tumor growth but also a significant reduction in cardiotoxic deaths compared with all the other co-administration groups and with the ADR-alone group in mice [14]. This remarkable finding has been subsequently studied in detail using mouse models [15, 16], and the reduction in toxic death was found to be DOC dose-dependent [16]; however, no

mechanism explaining the effect of DOC pre-administration has been established.

Proteomics is the large-scale study of gene expression at the protein level and provides information on dynamic cellular performance. As an integration of proteomics, toxicology, and bioinformatics, toxicoproteomics mainly focuses on protein changes in cells or tissues with exposure to toxicants, including antitumor drugs [17, 18].

In proteomic studies, comparative expression profiling of proteins has usually been performed using two-dimensional electrophoresis (2-DE) because this has been the method of choice. However, the 2-DE method has some drawbacks with regard to the reproducibility of the data. Importantly, 2-DE often cannot reproducibly resolve minute differences in protein expression levels between samples from different treatment groups. In an effort to overcome the limitation of 2-DE, Imai and colleagues developed an easily reproducible and highly sensitive proteomic approach, fluorogenic derivatization-liquid chromatography tandem mass spectrometry (FD-LC-MS/MS) method [19, 20]. This method involves fluorogenic derivatization of proteins, followed by high performance liquid chromatography (HPLC) of the derivatized proteins, isolation of those proteins with differential expression between the treatment groups, enzymatic digestion of the isolated proteins, and identification of the isolated proteins utilizing LC-tandem MS with a database-searching algorithm. This method enables highly sensitive detection and high resolution of proteins at the femtomol level due to the fluorogenic derivatization which utilizes a non-fluorescent reagent to yield highly fluorescent products. The applicability of the method has been demonstrated in the analyses of extracts from *Caenorhabditis elegans*, mouse liver, breast cancer cell lines, mouse

brain, and thoroughbred horse skeletal muscle, revealing the proteins related to early stage Parkinson's disease, hepatocarcinogenesis, metastatic breast cancer, aging, and training effects, respectively [21-26].

The aim of this study was to identify the cellular processes affected by the pre-administration of DOC in ADR/DOC combination therapies using a toxicoproteomic approach based on FD-LC-MS/MS. The present study reported the differential analysis of mouse heart tissues isolated from control, in intermittent-dosing (DOC-ADR), and simultaneous-dosing (ADR&DOC) groups.

2. Material and methods

2.1. Preparation of dosing drugs

ADR, supplied by Kyowa Hakko Kogyo Co., Ltd. (Tokyo, Japan), was dissolved in saline; the concentration was 2 mg/ml. DOC (Taxotere[®], Sanofi-aventis, Bridgewater, NJ, USA) was dissolved in ethanol; 5% glucose in water was added to obtain the ratio of ethanol and glucose solution (3:97, v/v) and the final concentration of DOC was 1.25 mg/ml

2.2 Animal treatment and tissue processing

Male ICR mice (5-weeks old) were purchased from Japan SLC (Nagasaki, Japan). Mice were housed 3-4 per cage under standardized light-dark cycle conditions (light on 7:00 to 19:00) at a room temperature of $24 \pm 1^\circ\text{C}$ with free access to food and water. Animal care and experimental procedures were performed in accordance with the Guide for the Care and

Use of Laboratory Animals (National Institute of Health) with approval from the Institutional Animal Care and Use Committee of Graduate School of Biomedical Sciences, Nagasaki University. Mice were divided into the intermittent-dosing group (DOC-ADR), in which ADR was administered 12 h after DOC injection; the simultaneous-dosing group (ADR&DOC), in which both drugs were administered simultaneously; and the saline-treated group (control), in which saline was administered at the same timing as ADR injection of the other groups. The anticancer drugs were intravenously administered once (20 mg/kg of ADR and 12.5 mg/kg of DOC) (Fig. 1). The ADR dose had been shown to be cardiotoxic in mouse [27]. The DOC dose had been shown to provide the strongest cardioprotection in the intermittent-dosing mouse group [16]. Also, when dosing intervals (6, 12, 24 h) between DOC and ADR treatments were changed, 12-h interval group showed the lowest toxic death rate [16]. Heart samples were isolated from all mice 1 week after ADR was administered in the ADR&DOC and DOC-ADR groups. All heart samples were immediately rinsed with phosphate buffer saline and frozen at -196°C . All heart samples were homogenated using the Frozen Cell Crasher (Microtec Co., Ltd., Chiba, Japan). At least four mice were used in each experimental group (i.e., control, DOC-ADR and ADR &DOC), and all data was subjected to statistical analysis.

2.3 Preparation of samples and determination of total proteins

Homogenated heart tissues (50 mg) were suspended in 250 μl of 10 mM 3-[(3-cholamidopropyl)dimethylammonio]propanesulfonate (CHAPS) solution (Dojindo

Laboratories, Kumamoto, Japan), and were centrifuged at 5000 g for 15 min at 4°C. The supernatant was then collected and stored as a soluble fraction at -80°C until use. The total protein content of the supernatant was determined with the Quick Start Bradford Protein assay kit (Bio-Rad Laboratory, Inc., Hercules, CA, USA) with bovine serum albumin as a standard protein by following the written instructions. After determination of total protein content, the supernatant was diluted with CHAPS solution to 2.4 mg total protein/ml and used as a starting protein sample.

2.4. FD-LC-MS/MS method

A 10- μ l volume of sample was mixed with 42.5 μ l of a mixture of 0.83 mM tris(2-carboxyethyl)phosphine hydrochloride (Tokyo Chemical Industry, Tokyo, Japan), 3.33 mM ethylenediamine-*N,N,N',N'*-tetraacetic acid (Dojindo Laboratories, Kumamoto, Japan), and 16.6 mM CHAPS in 6 M guanidine hydrochloride buffer solution (pH 8.7, Tokyo Chemical Industry, Tokyo, Japan). Then, this sample was subsequently mixed with 2.5 μ l of 140 mM 7-chloro-*N*-[2-(dimethylamino)ethyl]-2,1,3-benzoxadiazole-4-sulfonamide (DAABD-Cl, Tokyo Chemical Industry, Tokyo, Japan), which is the fluorogenic derivatization reagent, in acetonitrile (Merck KGaA, Darmstadt, Germany). After the reaction mixture was incubated in a 50°C water bath for 5 min, 1.5 μ l of 20% trifluoroacetic acid (TFA, Nacalai Tesque, Kyoto, Japan) was added to stop the derivatization reaction. A portion (20 μ l) of this reaction mixture (8.7 μ g protein) was injected into the HPLC-fluorescence detection system at a flow rate of 0.55 ml/min. The overall system

consisted of a Shimadzu Prominence series HPLC system (Kyoto, Japan) and a fluorescence detector (Shimadzu RF-10 A_xL; λ_{ex} . 395 nm; λ_{em} . 505 nm). The protein column (Intrada WP-RP, 250 x 4.6 mm i.d., Imtakt Co., Kyoto, Japan) was used as a stationary phase for separation of the derivatized proteins at a column temperature of 60°C. The mobile phase consisted of 0.1 % TFA in (A) water and (B) acetonitrile. The gradient elution was established with the following condition: 10% B held for 10 min; to 25% B in 30 min; to 28% B in 60 min; to 30% B in 80 min; to 31% B in 120 min; to 33% B in 190 min; to 34% B in 210 min; to 34.5% B in 230 min; to 39% B in 300 min; to 44.5% in 340 min. Corresponding peak heights were compared to identify differential protein profiles in the treatment groups.

Each subject protein in eluant recovered from the above HPLC system was concentrated to 5 μ l under reduced pressure and used for further identification process. The residue was diluted with 240 μ l of 50 mM ammonium bicarbonate solution (pH 7.8) (Nacalai Tesque, Kyoto, Japan), 5 μ l of 10 mM calcium chloride (Nacalai Tesque, Kyoto, Japan), and 5 μ l of 20 ng / μ l trypsin (Promega, Wisconsin, WI, USA), and the resultant mixture was incubated for 2 h at 37°C. This mixture was then concentrated to 20 μ l under reduced pressure.

The peptide mixture (2 μ l) was subjected to an LC-electrospray ionization-tandem MS (LCQ Fleet, Thermo Fisher Scientific, Waltham, MA, USA) equipped with the custom nanoLC system consisting of a typical LC pump (Surveyor MS pump, Thermo Fisher Scientific, Waltham, MA, USA) with LC flow splitter (Accurate, Dionex, Sunnyvale, CA, USA) and an HCT PAL autosampler (CTC Analytics, Zwingen, Switzerland). The sample

was loaded onto a nano-precursor column (300 μm i.d. x 5.0 mm, C₁₈PepMap, Dionex, Sunnyvale, CA, USA) in the injection loop and washed using 0.1% TFA in 2% acetonitrile. Peptides were separated and ion-sprayed into MS by a nano HPLC column (75 μm i.d., 3 μm C₁₈ packed 12 cm, Nikkyo Technos, Tokyo, Japan) with a spray voltage from 1.2 to 2.0 kV. Separation was performed, employing a gradient from 5 to 50% mobile phase B (0.1% formic acid [Kanto Kagaku, Tokyo, Japan] in 90% acetonitrile) over a period of 30 min (mobile phase A: 0.1% formic acid); 50 to 100% mobile phase B in 30.1 min; 100% mobile phase B held for 10 min. The mass spectrometer was configured to optimize the duty cycle length with the quality of data acquired by progressing from a full scan of the sample to three tandem MS scans of the three most intense precursor masses (as determined by Xcaliber[®] software [Thermo Fisher Scientific, Waltham, MA, USA] in real time). The collision energy was normalized to 35%. All the spectra were measured with an overall mass/charge ratio range of 400-1500. The transfer capillary temperature was set at 200°C. MS/MS data were extracted using Bioworks v.3.3 (Thermo Fisher Scientific, Waltham, MA, USA). Spectra were searched against a murine subdatabase from the public non-redundant protein database of the National Center for Biotechnology Information (NCBI, Bethesda, MD, USA) (download date: July 16, 2009) with the following search parameters: mass type, monoisotopic precursor and fragments; enzyme, trypsin (KR); enzyme limits, full enzymatic cleavage allowing up to two missed cleavages; peptide tolerance, 2.0 atomic mass units; fragment ion tolerance, 1.0 atomic mass unit; number of results scored, 250; ion and ion series calculated, B and Y ions; static modification, C (fluorogenic derivatization); differential

modifications, M (oxidation), N and Q (deamidation). The filter criteria (single, double, and triple charge peptides with a correlation factor [XCorr] and protein probability [P]) were adjusted keeping the empirically determined protein false discovery rate (FDR) below 1.0%. FDR was calculated using the number of significant unique peptide in the reversed database divided by the number of those in the forward database. Proteins were identified with more than two peptides ≥ 6 amino acids long. A low probability suggests a good match in that it indicates that the match between the sequence and the spectrum could not easily happen by accident. If multiple proteins shared amino acid sequences with found peptides, the protein with the lowest probability among them was determined to be the most likely match, and ubiquitous keratins and trypsin were excluded as potential matches.

2.5. Statistical analysis

Results are expressed as the mean \pm standard deviation. Differences between the groups were determined by Tukey-Kramer multiple comparison test. $P < 0.05$ was considered to be significant.

3. Results

3.1. Analytical performance of FD-LC-MS/MS method

The total protein amount required for quantification was 8.7 μg per HPLC injection. The precision of the method was confirmed based on the reproducibility of the peak heights using four peaks, including high, medium, and low peaks. The relative standard deviation

(RSD, %) values were in the range of 6.6-11.9% for between-days (n = 5) replicates. The reproducibility of the retention times using same peaks was also calculated, and the between-day RSD values were less than 0.82% (n = 5).

3.2. Differential profiling and protein identification

Typical chromatograms from FD-LC-MS/MS analysis of DOC-ADR and ADR&DOC samples are depicted in Fig. 2. Each peak height shows the expression level of an individual protein. Twenty-five protein peaks (Table 1) appeared to differ but nine proteins differed with statistical significance at the *P* levels shown in Fig. 3. Also, the differences in the expression levels of these proteins, group according to their functional classification, are depicted in Fig. 3. The peak numbers of the differentially expressed proteins are inserted in Fig. 2. In both of the drug treatment groups, aconitase (peak no. 11) and lactate dehydrogenase A (Ldha) protein (peak no. 23) were significantly reduced and ubiquinol-cytochrome c reductase (peak no. 7) was significantly elevated relative to the control group. The expression of glyceraldehyde-3-phosphate dehydrogenase (GAPDH, peak no. 13) in the DOC-ADR group increased more than 7-fold, compared with the ADR&DOC group. Creatine kinase (CK) was significantly increased in the DOC-ADR group, compared with the control.

4. Discussion

In our pre-clinical (mouse) study [14], the DOC-ADR group showed a significantly

higher survival rate compared with the ADR&DOC group ($P < 0.01$), and the survival rates on day 35 were 86.2% in the DOC-ADR group and 22.2% in the ADR&DOC group. A subsequent study revealed that the toxic death of mouse was attributed to cardiotoxicity induced by ADR [16]. Therefore, in this study, the differential proteomic profiling of mouse heart tissues from DOC-ADR, ADR&DOC, and control groups was performed to identify the proteins that mediate the cardioprotective effect of DOC pretreatment in the DOC-ADR group. Significant QT interval prolongation of mouse was observed 1 week after ADR-treatment, compared with non-treated mouse; therefore, 1 week after drug treatment was chosen for the toxicoproteomic analysis.

The RSD values suggest that the FD-LC-MS/MS method has an excellent reproducibility in the proteomic analysis of heart tissue samples. With the FD-LC-MS/MS method, reproducible chromatograms were obtained from heart tissue with small amounts of protein (8.7 μg per HPLC injection), in contrast to other proteomic methods where from dozens to hundreds of micrograms of protein samples are required [28, 29]. The fluorogenic derivatization is cysteine thiol-specific. The fluorogenic reagent (DAABD-Cl) is excessively added to the sample; therefore, all the proteins with one or more cysteine residues are labeled and are able to be detected by fluorescence detector. The cysteine-free proteins are excluded from the analytical targets of FD-LC-MS/MS; however, most of proteins contain one or more cysteine residues [30] and other proteomic methods with labeling technologies, such as isotope-coated affinity tag (ICAT) targeting cysteine thiol, have been widely applied to proteomic studies [31, 32]. For the sensitivity of FD-LC-MS/MS, the detection limit of an

actin standard (MW 43000, including 6 cysteine residues) was 440 femtomol per HPLC injection [24]. The sensitivities of different proteins with similar molecular weight are considered to be partly dependent on the number of cysteine included in the protein.

Based on the high sensitivity, resolution, and reproducibility, nine proteins were found to be differentially expressed between the three groups, seven of which were the proteins involved in energy production processes, the glycolytic pathway, the tricarboxylic acid (TCA) cycle, and the electron transport chain as shown in Fig. 3. Among the differentially expressed proteins, aconitase (peak no. 11) was the most drastically reduced in this study and has been reported to be inactivated by ADR treatment [33, 34]. Also, Ldha protein (peak no. 23) was significantly decreased in both drug treatment groups when compared with the control. Lactate dehydrogenase is known as an escape enzyme that reflects cytotoxicity or cellular damage and has been measured in toxicological studies. Therefore, these results ensured the validity of FD-LC-MS/MS as a toxicoproteomic method.

Most of the differentially expressed proteins identified in our study are involved in the myocardial energy network. Heart muscle requires large amounts of energy to sustain its contractile performance; therefore, cellular energy deficits are recognized as an important and common factor in the development of cardiac myopathies [35-37]. Adenosine 5'-triphosphate (ATP) serves as primary, immediate source of energy; however intracellular ATP pools are rather small. Moreover, ADR have been reported to diminish cardiac energy reserves by reducing ATP through several mechanisms, such as oxidative damage, damage to membrane and signaling pathways, disruption of mitochondria function, and inflammation

[38-42]. These effects have been consistently observed in patients treated with ADR [43]. Evidence has accumulated indicating a relationship between myocardial energy metabolism and ADR-induced cardiotoxicity [44].

Among the six proteins that were differently expressed between the dosing groups, four were more highly expressed in the ADR&DOC group than in the DOC-ADR group (peak nos. 10, 11, 16, and 19). Based on their high expression levels in the ADR&DOC group, it was assumed that the activated energy production contributed to enhance cardiac contractile force and maintain the function. However, the elevated expression observed in the ADR&DOC group did not lead to an increase in survival rate in the combination therapy. In other words, the lower expression of the four proteins in the DOC-ADR group did not adversely affect survival. Furthermore, although the expression of TCA cycle enzymes (peak nos. 11 and 16) in the DOC-ADR group was significantly lower than those in control group, a higher survival rate was observed in DOC-ADR group than in the ADR&DOC and ADR-only treatment groups [14, 16]. Therefore, the alteration of these four proteins may not be a definitive factor for cardioprotective effect of DOC-pretreatment.

GAPDH catalyses the nicotinamide adenine dinucleotide-dependent conversion of glyceraldehyde-3-phosphate into 1,3 -diphosphoglycerate. It is the first energy-harvesting enzyme and a central player in glycolytic pathway, placing it at the core of cancer cell survival [45]. Generally, GAPDH is considered a housekeeping enzyme because it is constitutively expressed in most tissues and cell types. However, several reports revealed that it is differentially regulated by circadian clock or in disease states [46, 47]. The highly

elevated expression of GAPDH in the DOC-ADR group may be important in maintaining cardiac function after combination therapy and result in higher survival rates. It is unclear whether all glycolysis-dependent energy supply is increased by elevated expression of GAPDH because the expression of another glycolytic enzyme, aldolase, was lower in the DOC-ADR group than in the ADR&DOC group. However, it was reported that ADR induced a decrease in ATP content in endothelial cell, which was paralleled by a decrease in GAPDH activity [48]. Therefore, to some extent, the elevated expression of GAPDH in the DOC-ADR group might protect heart muscle from ADR-induced cardiotoxicity. The cardiotoxicity of ADR has been ascribed mainly to oxidative stress by ADR-induced free radicals predominantly accumulating in mitochondria. It is possible that the elevated expression of GAPDH is a result of the compensatory activation of energy supply via a glycolytic pathway, responding to severe reductions in mitochondrial ATP production due to the accumulation of ADR-induced free radicals. Alternatively, Baek *et al.* proposed direct scavenging of reactive oxygen species (ROS) by GAPDH based on the result that over-expression of GAPDH in yeast cells resulted in an increase in overall cellular antioxidative capacity [49]. Because ROS are involved in Bax-induced apoptosis in yeast and plants [50], ROS-induced cell death in animals might be inhibited by GAPDH. Moreover, a variety of recent studies have brought new insights into this old enzyme, and current evidence now suggests that GAPDH is a multifunctional protein that is involved in numerous cellular processes in animals [51-55]; therefore, unknown effects of GAPDH may contribute to the cardioprotective effects of DOC pre-administration in ADR/DOC

combination therapies.

CK catalyses the reversible conversion of phosphocreatine and adenosine diphosphate to creatine and ATP. The elevated expression of CK may indicate a relatively high cellular energy state in the DOC-ADR group relative to the control group; although the expression was found not to be significantly different between the two dosing groups.

To date, two papers have reported proteomic studies of ADR-induced cardiotoxicity and the mechanism against it [56, 57]. On one hand, redox proteomics was performed based on the hypothesis that the cardiotoxic actions of ADR are caused by the oxidative stress [56]. However, that approach may be insufficient to reveal alterations in protein expression in important cellular processes because it focuses on identifying only the oxidatively modified proteins. Using a different approach, Kang and colleagues identified differences in global proteomic profiles of heart tissue between non-transgenic (TG) and TG mice that over-express metallothionein to understand the molecular mechanism of metallothionein protection against ADR-induced cardiotoxicity [57]. They found elevated expression of cytochrome c oxidase subunit Va, which regulates oxidative phosphorylation, in TG mouse heart in response to ADR treatment. In the present study, the highly sensitive proteomic analysis of heart tissues suggests that GAPDH may counteract ADR-induced cardiotoxicity. GAPDH is a multifunctional protein, participating in energy supply and antioxidative activity; therefore any or all of GAPDH's functions may be relevant to the cardioprotective effects observed in the DOC-ADR treatment group. However, it was not yet clear exactly what mechanism was responsible for either the cardioprotective effects or the over-expression of GAPDH observed

in the DOC-ADR group. Previous research has shown that the over-expression of antioxidant enzymes (*i.e.*, superoxide dismutase and catalase) in TG mice protected heart from ADR-induced cardiotoxicity [58, 59]. Therefore, the same transgenic approach or another approach with the addition of *N*⁶-naphthalenemethyl-2'-methoxybenzamido- β -NAD⁺ for GAPDH inhibition [60] may be useful in validating and elucidating any cardioprotective effects associated with GAPDH. Further analysis of GAPDH is necessary to determine if it is a potential target for protective intervention against ADR-induced cardiotoxicity.

In summary, in order to better understand the cardioprotective effect of pre-administration of DOC in an ADR/DOC combination anti-cancer therapy, we applied the FD-LC-MS/MS method to differential proteomic analysis of heart tissues from control, intermittent-dosing and simultaneous-dosing groups of mice. This highly reproducible and sensitive method identified significantly altered expression of nine proteins in mouse heart, and seven of these proteins are involved in the cellular energy production. Significantly elevated expression of GAPDH was observed in the DOC-ADR group, in which the survival rate was higher [14, 16], than the ADR&DOC group. Therefore, GAPDH may be developed as a potential target for protective intervention and a biomarker for evaluation of cardioprotective effect of experimental treatments in pre-clinical studies.

Acknowledgement

K. O. is grateful to the support provided by the Special Coordination Funds for Promoting Science and Technology of the Ministry of Education, Culture, Sports, Science and

Technology (MEXT). We also acknowledge the technical support of Mr. Daisuke Higo (Thermo Fisher Scientific) in the protein identification.

The authors declared no conflict of interest.

References

- [1] Buzdar AU, Marcus C, Smith TL, Blumenschein GR. Early and delayed clinical cardiotoxicity of doxorubicin. *Cancer* 1985; 55: 2761-2765.
- [2] Bontenbal M, Creemers G-J, Braun HJ, de Boer AC, Janssen J Th, Leys RB, Ruit JB, Goey SH, van der Delden PC, Kerkhofs LG, Schothorst KL, Schmitz PI, Bokma HJ, Verweij J, Seynaeve C. Phase II to III study comparing doxorubicin and docetaxel with fluorouracil, doxorubicin, and cyclophosphamide as first-line chemotherapy in patients with metastatic breast cancer: Results of a Dutch community setting trial for the clinical trial group of the comprehensive cancer center. *J Clin Oncol* 2005; 23: 7081-7088.
- [3] Nabholz JM, Falkson C, Campos D, Szanto J, Martin M, Chan S, Pienkowski T, Zaluski J, Pinter T, Krzakowski M, Vorobiof D, Leonard R, Kennedy I, Azli N, Murawsky M, Riva A, Pouillart P. Docetaxel and doxorubicin compared with doxorubicin and cyclophosphamide as first-line chemotherapy for metastatic breast cancer: results of a randomized, multicenter, phase III trial. *J Clin Oncol* 2003; 21: 968-975.
- [4] Mattioli R, Lippe P, Massacesi C, Cappelletti C, Nacciarriti D, Bissoni R, Graziano F, Menichetti ET, Imperatori L, Testa E, Lenci G, Balletta A, Silva RR. Long-survival in responding patients with metastatic breast cancer treated with doxorubicin-docetaxel combination. A multicenter phase II trial. *Anticancer Res* 2004; 24: 3257-3262.
- [5] Lévi F, Zidani R, Misset J. Randomized multicenter trial of chronotherapy with oxaliplatin, fluorouracil, and folic acid in metastatic colorectal cancer. *International Organization for Cancer Chronotherapy. Lancet* 1997; 350: 681-686.

- [6] Kobayashi M, To H, A. Tokue A, Fujimura A, Kobayashi E. Cisplatin-induced vomiting depends on circadian timing. *Chronobiol Int* 2001; 18: 851-863.
- [7] To H, Kikuchi A, Tsuruoka S, Sugimoto K, Fujimura A, Higuchi S, Kayama F, Hara K, Matsuno K, Kobayashi E. Time-dependent nephrotoxicity associated with daily administration of cisplatin in mice. *J Pharm Pharmacol* 2000; 52: 1499-1504.
- [8] Hrushesky WJ. Circadian timing of cancer chemotherapy. *Science* 1985; 228: 73-75.
- [9] Tampellini M, Filipinski E, Liu XH, Lemaigre G, Li XM, Francois E, Bissery MC, Lévi F. Docetaxel chronopharmacology in mice. *Cancer Res* 1998; 58: 3896-3904.
- [10] To H, Ohdo S, Shin M, Uchimarui H, Yukawa E, Higuchi S, Fujimura A, Kobayashi E. Dosing-time dependency of adriamycin-induced cardiotoxicity and bone marrow toxicity in rats. *J Pharm Pharmacol* 2003; 55: 803-810.
- [11] Lévi F, Halberg F, Haus E. Synthetic adrenocorticotropin for optimizing murine circadian chronotolerance for adriamycin. *Chronobiologia* 1980; 7: 227-244.
- [12] Scheving LE, Burns ER, Pauly JE, Halberg F. Circadian bioperiodic response of mice bearing advanced L1210 leukemia to combination therapy with adriamycin and cyclophosphamide. *Cancer Res* 1980; 40: 1511-1515.
- [13] Barrett RJ, Blessing JA, Homesley HD, Twigg L, Webster KD. Circadian-timed combination doxorubicin-cisplatin chemotherapy for advanced endometrial carcinoma. A phase II study of the Gynecologic Oncology Group. *Am J Clin Oncol* 1993; 16: 494-496.
- [14] To H, Shin M, Tabuchi M, Sakaguchi H, Takeuchi A, Matsunaga N, Higuchi S, Ohdo S. Influence of dosing schedule on toxicity and antitumor effects of a combination of adriamycin

and docetaxel in mice. *Clin Cancer Res* 2004; 10: 762-769.

[15] Tabuchi M, To H, Sakaguchi H, Goto N, Takeuchi A, Higuchi S, Ohdo S. Therapeutic index by combination of adriamycin and docetaxel depends on dosing time in mice. *Cancer Res* 2005; 65: 8448-8454.

[16] Sakaguchi H, Kodama A, Tomonari M, Ando Y, Tabuchi M, To H, Araki R, Kitahara T, Sasaki H, Higuchi S, Ohdo S. Pre-administration of docetaxel protects against adriamycin-induced cardiotoxicity. *Breast Cancer Res Treat* 2008; 109: 443-450.

[17] Ge Y, Preston RJ, Owen RD. Toxicoproteomics and its application to human health risk assessment. *Proteomics Clin Appl* 2007; 1: 1613-1624.

[18] Bandara LR, Kennedy S. Toxicoproteomics-a new preclinical tool. *Drug Discov Today* 2002; 7: 411-418.

[19] Toriumi C, Imai K. An identification method for altered proteins in tissues utilizing fluorogenic derivatization, liquid chromatography, tandem mass spectrometry, and a database searching algorithm. *Anal Chem* 2003; 75: 3725-3730.

[20] Masuda M, Toriumi C, Santa T, Imai K. Fluorogenic derivatization reagents suitable for isolation and identification of cysteine-containing proteins utilizing high-performance liquid chromatography-tandem mass spectrometry. *Anal Chem* 2004; 76: 728-735.

[21] Masuda M, Saimaru H, Takamura N, Imai K. An improved method for proteomic studies on *C. elegans* by fluorogenic derivatization, HPLC isolation, enzymatic digestion, and liquid chromatography-tandem mass spectrometric identification. *Biomol Chromatogr* 2005; 19: 556-560.

- [22] Ichibangase T, Saimaru H, Takamura N, Kuwahara T, Koyama A, Iwatsubo T, Imai K. Proteomics of *Caenorhabditis elegans* over-expressing human alpha-synuclein analyzed by fluorogenic derivatization-liquid chromatography/tandem mass spectrometry: identification of Actin and several ribosomal proteins as negative markers at early Parkinson's disease stages. *Biomed Chromatogr* 2008; 22: 232-234.
- [23] Ichibangase T, Moriya K, Koike K, Imai K. A proteomic method revealing disease-related proteins in livers of hepatitis-infected mouse model. *J Proteome Res* 2007; 6: 2841-2849.
- [24] Imai K, Ichibangase T, Saitoh R, Horikawa Y. A proteomics study on human breast cancer cell lines by fluorogenic derivatization-liquid chromatography-tandem mass spectrometry. *Biomed Chromatogr* 2008; 22: 1304-1314.
- [25] Asamoto H, Ichibangase T, Uchikuro K, Imai K. Application of an improved proteomics method, fluorogenic derivatization-liquid chromatography-tandem mass spectrometry, to differential analysis of proteins in small regions of mouse brain. *J Chromatogr A* 2008; 1208: 147-155.
- [26] Ichibangase T, Imai K. Application of fluorogenic derivatization-liquid chromatography-tandem mass spectrometric proteome method to skeletal muscle proteins in fast thoroughbred horses. *J Proteome Res* 2009; 8: 2129-2134.
- [27] Nozaki N, Shishido T, Takeishi Y, Kubota I. Modulation of doxorubicin-induced cardiac dysfunction in toll-like receptor-2-knockout mice. *Circulation* 2004; 110: 2869-2874.
- [28] Wu WW, Wang G, Baik SJ, Shen RF. Comparative study of three proteomic quantitative

methods, DIGE, cICAT, and iTRAQ, using 2D gel- or LC-MALDI TOF/TOF. *J Proteome Res* 2006; 5: 651-658.

[29] Qu J, Jusko WJ, Straubinger R M. Utility of cleavable isotope-coated affinity-tagged reagents for quantification of low-copy proteins induced by methylprednisolone using liquid chromatography / tandem mass spectrometry. *Anal Chem* 2006; 78: 4543-4552.

[30] Miseta A, Csutora P. Relationship between the occurrence of cysteine in proteins and the complexity of organism. *Mol Biol Evol* 2000; 17: 1232-1239.

[31] Welch KD, Wen B, Goodlett DR, Yi E, Lee H, Reilly T, Nelson SD, Pohl LR. Proteomic identification of potential susceptibility factors in drug-induced liver disease. *Chem Res Toxicol* 2005; 18: 924-933.

[32] Hirsch J, Hansen KC, Choi S, Noh J, Hirose R, Roberts J, Matthay MA, Burlingame AL, Maher JJ, Niemann CU. Warm ischemia-induced alterations in oxidative and inflammatory proteins in hepatic kupffer cells in rats. *Mol Cell Proteomics* 2006; 5: 979-986.

[33] Turakhia S, Venkatakrishnan CD, Dunsmore K, Wong H, Kuppusamy P, J.L. Zweier JL, G. Ilangoan G. Doxorubicin-induced cardiotoxicity: direct correlation of cardiac fibroblast and H9c2 cell survival and aconitase activity with heat shock protein 27. *Am J Physiol Heart Circ Physiol* 2007; 293: 3111-3121.

[34] Sacco G, Giampietro R, Salvatorelli E, Menna P, Bertani N, Graiani G, Animati F, Goso C, Maggi CA, Manzini S, Minotti G. Chronic cardiotoxicity of anticancer anthracyclines in the rat: role of secondary metabolites and reduced toxicity by a novel anthracycline with impaired metabolite formation and reactivity. *Br J Pharmacol* 2003; 139: 641-651.

- [35] Dzeja PP, Redfield MM, Burnett JC, Terzic A. Failing energetics in failing hearts. *Curr Cardiol Rep* 2000; 2: 212-217.
- [36] Ingwall JS, Weiss RG. Is the failing heart energy starved? On using chemical energy to support cardiac function. *Circ Res* 2004; 95: 135-146.
- [37] Ventura-Clapier R, Garnier A, Veksler V. Energy metabolism in heart failure. *J Physiol* 2004; 555: 1-13.
- [38] Wallace KB. Doxorubicin-induced cardiac mitochondriopathy. *Pharmacol Toxicol* 2003; 93: 105-115.
- [39] Jayaseelan R, Poizat C, Wu HY, Kedes L. Molecular mechanisms of doxorubicin-induced cardiomyopathy. *J Biol Chem* 1997; 272: 5828-5832.
- [40] Zhou S, Heller LJ, Wallace KB. Interference with calcium-dependent mitochondrial bioenergetics in cardiac myocytes isolated from doxorubicin-treated rats. *Toxicol Appl Pharmacol* 2001; 175: 60-67.
- [41] Bruynzeel A, Abou El Hassan MA, Schalkwijk C, Berkhof J, Bast A, Niessen HWM, van der Vijgh WJF. Anti-inflammatory agents and monoHER protect against DOX-induced cardiotoxicity and accumulation of CML in mice. *Br J Cancer* 2007; 96: 937-943.
- [42] A. Riad A, S. Bien S, D. Westermann D, P.M. Becher PM, K. Loya K, U. Landmesser U, H.K. Kroemer HK, H.P. Schultheiss HP, Tschoepe C. Pretreatment with statin attenuates the cardiotoxicity of doxorubicin in mice. *Cancer Res* 2009; 69: 695-699. 9
- [43] Eidenschink AB, Schroter G, Muller-Weihrich S, Stern H. Myocardial high-energy phosphate metabolism is altered after treatment with anthracycline in childhood. *Cardiol*

Young 2000; 10: 610-617.

[44] Tokarska-Schlattner M, Zaugg M, Zuppinger C, Wallimann T, Schlattner U. New insights into doxorubicin-induced cardiotoxicity: The critical role of cellular energetics. *J Mol Cell Cardiol* 2006; 41: 389-405.

[45] Phadke MS, Krynetskaia NF, Mishra AK, Krynetskiy E. Glyceraldehyde 3-phosphate dehydrogenase depletion induces cell cycle arrest and resistance to antimetabolites in human carcinoma cell lines. *J Pharmacol Exp Ther* 2009; 331: 77-86.

[46] Shinohara ML, Loros JJ, Dunlap JC. Glyceraldehyde-3-phosphate dehydrogenase is regulated on a daily basis by the circadian clock. *J Biol Chem* 1998; 273: 446-452

[47] Beisswenger PJ, Howell SK, Smith K, Zwergold BS. Glyceraldehyde-3-phosphate dehydrogenase activity as an independent modifier of methylglyoxal levels in diabetes. *Biochim Biophys Acta Mol Basis Dis* 2003; 1637: 98-106.

[48] Wolf MB, Baynes JW. The anti-cancer drug, doxorubicin, causes oxidant stress-induced endothelial dysfunction. *Biochim Biophys Acta* 2006; 1760: 267-271.

[49] Baek D, Jin Y, Jeong JC, Lee HJ, Moon H, Lee J, Shin D, Kang CH, Kim DH, Nam J, Lee SY, Yun DJ. Suppression of reactive oxygen species by glyceraldehyde-3-phosphate dehydrogenase. *Phytochemistry* 2008; 69: 333-338.

[50] Kawai-Yamada M, Jin L, Yoshinaga K, Hirata A, Uchimiya H. Mammalian Bax inhibitor-1 suppressing Bax-, hydrogen peroxide-, and salicylic acid-induced cell death. *Plant Cell* 2004; 16: 21-32.

[51] Sirover MA. New nuclear functions of the glycolytic protein,

glyceraldehyde-3-phosphate dehydrogenase, in mammalian cells. *J Cell Biochem* 2005; 95: 45-52.

[52] Colell A, Ricci JE, Tait S, Milasta S, Maurer U, Bouchier-Hayes L, Fitzgerald P, Guio-Carrion A, Waterhouse NJ, Li CW, Mari B, Barbry P, Newmeyer DD, Beere HM, Green DR. GAPDH and autophagy preserve survival after apoptotic cytochrome c release in the absence of caspase activation. *Cell* 2007; 129: 983-997.

[53] Zhang L, Roeder RG, Luo Y. S phase activation of the histone H2B promoter by OCA-S, a coactivator complex that contains GAPDH as a key component. *Cell* 2003; 114: 255-266.

[54] Hara MR, Agrawal N, Kim SF, Cascio MB, Fujimuro M, Ozeki Y, Takahashi M, Cheah JH, Tankou SK, Hester LD, Ferris CD, Hayward SD, Snyder SH, Sawa A. S-nitrosylated GAPDH initiates apoptotic cell death by nuclear translocation following Siah1 binding. *Nat Cell Biol* 2005; 7: 665-674.

[55] Hara MR, Thomas B, Cascio MB, Bae BI, Hester LD, Dawson VL, Dawson TM, Sawa A, Snyder SH. Neuroprotection by pharmacologic blockage of the GAPDH death cascade. *Proc Natl Acad Sci USA* 2006; 103: 3887-3889.

[56] Chen Y, Daosukho C, Opii WO, Turner DM, Pierce WM, Klein JB, Vore M, Butterfield DA, Clair DKSt. Redox proteomic identification of oxidized cardiac proteins in adriamycin-treated mice. *Free Radic Biol Med* 2006; 41: 1470-1477.

[57] Merten KE, Feng W, Zhang L, Pierce W, Cai J, Klein JB, Kang YJ. Modulation of cytochrome c oxidase-Va is possibly involved in metallothionein protection from doxorubicin cardiotoxicity. *J Pharmacol Exp Ther* 2005; 315: 1314-1319.

[58] Yen HC, Oberley TD, Vichitbandha S, Ho YS, Clair DKSt. The protective role of manganese superoxide dismutase against adriamycin-induced acute cardiac toxicity in transgenic mice. *J Clin Invest* 1996; 98: 1253-1260.

[59] Kang YJ, Sun XH, Chen Y, Zhou ZX. Inhibition of doxorubicin chronic toxicity in catalase-overexpressing transgenic mouse heart. *Chem Res Toxicol* 2002; 15: 1-6.

[60] Kennedy KJ, Bressi JC, Gelb MH. A di-substituted NAD⁺ analogue is a nanomolar inhibitor of trypanosomal glyceraldehydes-3-phosphate dehydrogenase. *Bioorg Med Chem Lett* 2001; 11: 95-98.

Figure captions

Fig. 1 Experimental protocol and time-line for the *in vivo* studies. Abbreviations: DOC, docetaxel (12.5 mg/kg i.v.); ADR, adriamycin (20 mg/kg i.v.). Heart tissue sampling: animal sacrifice, removal heart and processing.

Fig. 2 Chromatograms of proteins derivatized with DAABD-Cl in mouse heart. The upper and lower chromatograms were obtained from the DOC-ADR and ADR&DOC groups, respectively. The peaks of differentially expressed proteins are numbered.

Fig. 3 Changes in peak heights relative to control between DOC-ADR and ADR&DOC groups. Peak numbers correspond to those in Fig. 2. Mean values \pm SD are plotted. Significant differences between control vs each dosing group are indicated by $^{\dagger}P \leq 0.05$ or $^{\dagger\dagger}P \leq 0.01$. Significant differences between DOC-ADR and ADR&DOC are indicated by $*P \leq 0.05$ or $**P \leq 0.01$.

Table 1 List of proteins identified by FD-LC-MS/MS method

Peak number ^a	Protein name	Molecular mass (Da)	SEQUEST score	Peptide hit	Coverage by mass	GI number ^b
1	Ecotropic viral integretion site 1	115594.0	18.1	3	1.28	gi 6679705
2	Superoxide dismutase 1, soluble	15932.8	54.2	6	35.66	gi 45597447
3	Actin, gamma, cytoplasmic 1	41765.8	18.1	2	5.30	gi 6752954
4	Diazepam binding inhibitor	9994.1	20.2	2	34.33	gi 22135646
5	Heterogeneous nuclear ribonucleoprotein A2/B1	35942.8	30.2	4	12.73	gi 219519440
6	Phosphatidylethanolamine binding protein 1	20817.3	18.2	2	12.20	gi 84794552
7	Ubiquinol-cytochrome c reductase, Rieske iron-sulfur polypeptide 1	29349.2	18.2	2	8.57	gi 18044191
8	Hemoglobin alpha 1 chain	15075.8	10.2	2	10.15	gi 6680175
9	Albumin	68647.8	74.2	10	11.08	gi 29612571
10	Aldolase A, fructose-bisphosphate	39331.3	42.3	5	8.46	gi 58477282
11	Aconitase 2, mitochondria	85444.1	110.3	13	13.24	gi 63101587
12	Myoglobin	17059.0	112.2	15	45.66	gi 19263902
13	Glyceraldehyde-3-phosphate dehydrogenase	35787.2	46.2	5	14.50	gi 148877869
14	Creatine kinase, muscle	43017.8	74.2	10	17.45	gi 124376420
15	Acetyl-coenzyme A acyltransferase 2 (mitochondrial 3-oxoacyl-Coenzyme A thiolase)	41831.5	34.2	4	14.56	gi 20810027
16	Isocitrate dehydrogenase 2 (NADP+), mitochondrial	50874.0	30.2	3	7.66	gi 37748684
17	Malate dehydrogenase 2, NAD (mitochondrial)	35585.8	48.2	5	14.93	gi 19484047
18	Electron transferring flavoprotein, alpha polypeptide	34987.5	28.2	4	5.44	gi 66911229
19	Electron transferring flavoprotein, alpha polypeptide	34987.5	30.2	3	12.44	gi 66911229
20	Enolase 3, beta muscle	46995.3	40.2	6	9.11	gi 15488630
21	Acyl-Coenzyme A dehydrogenase, long chain	47877.5	20.2	2	5.40	gi 20071667
22	Pyruvate dehydrogenase (lipoamide) beta	38912.1	30.2	4	14.78	gi 63101525
23	Ldha protein	36475.2	18.1	2	3.43	gi 111598933
24	Lactate dehydrogenase B	36549.1	54.2	6	17.00	gi 28386162
25	Malate dehydrogenase 1, NAD (soluble)	36488.1	38.2	4	15.26	gi 37589957

^aPeak numbers correspond to those in Fig. 2. ^bGI number is simply a series of digits that are assigned consecutively to each sequence record

processed by NCBI.

Fig. 1

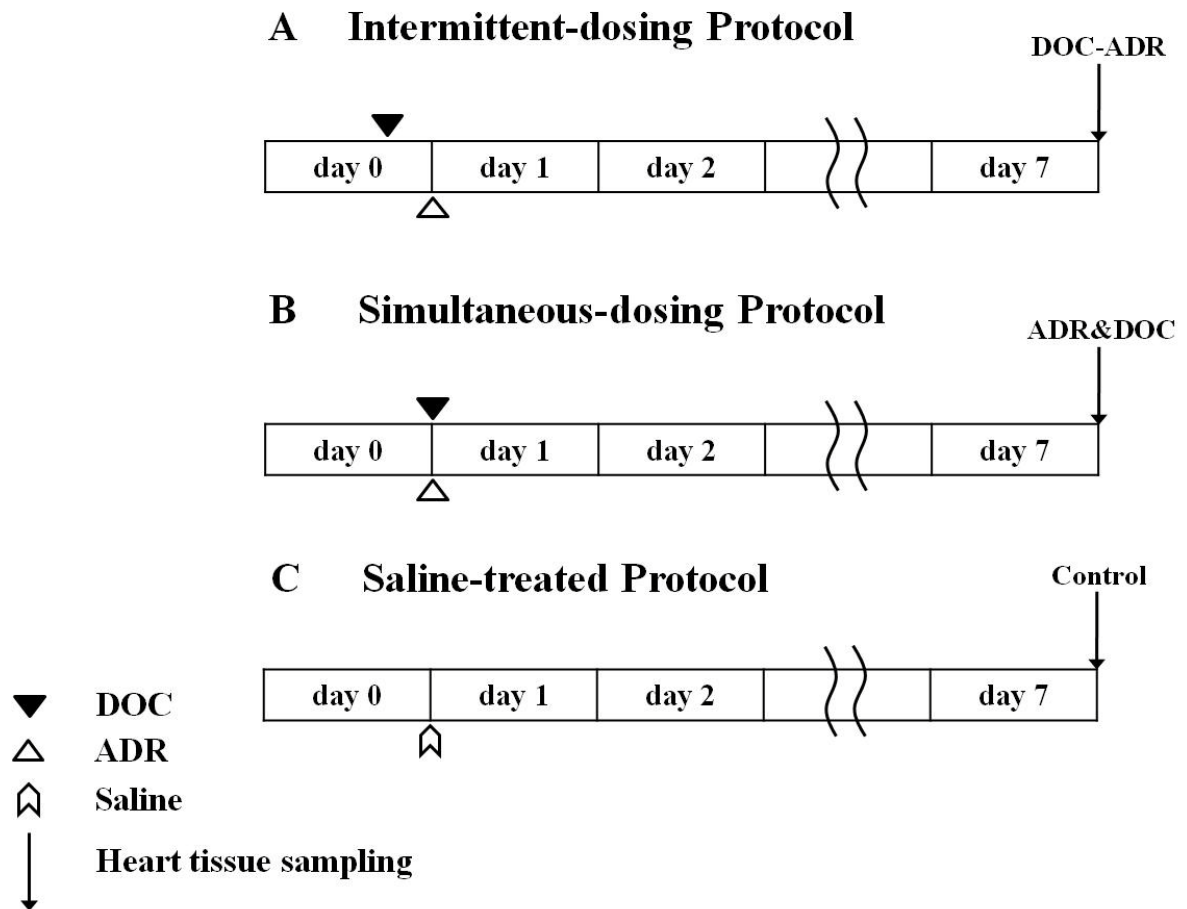


Fig. 2

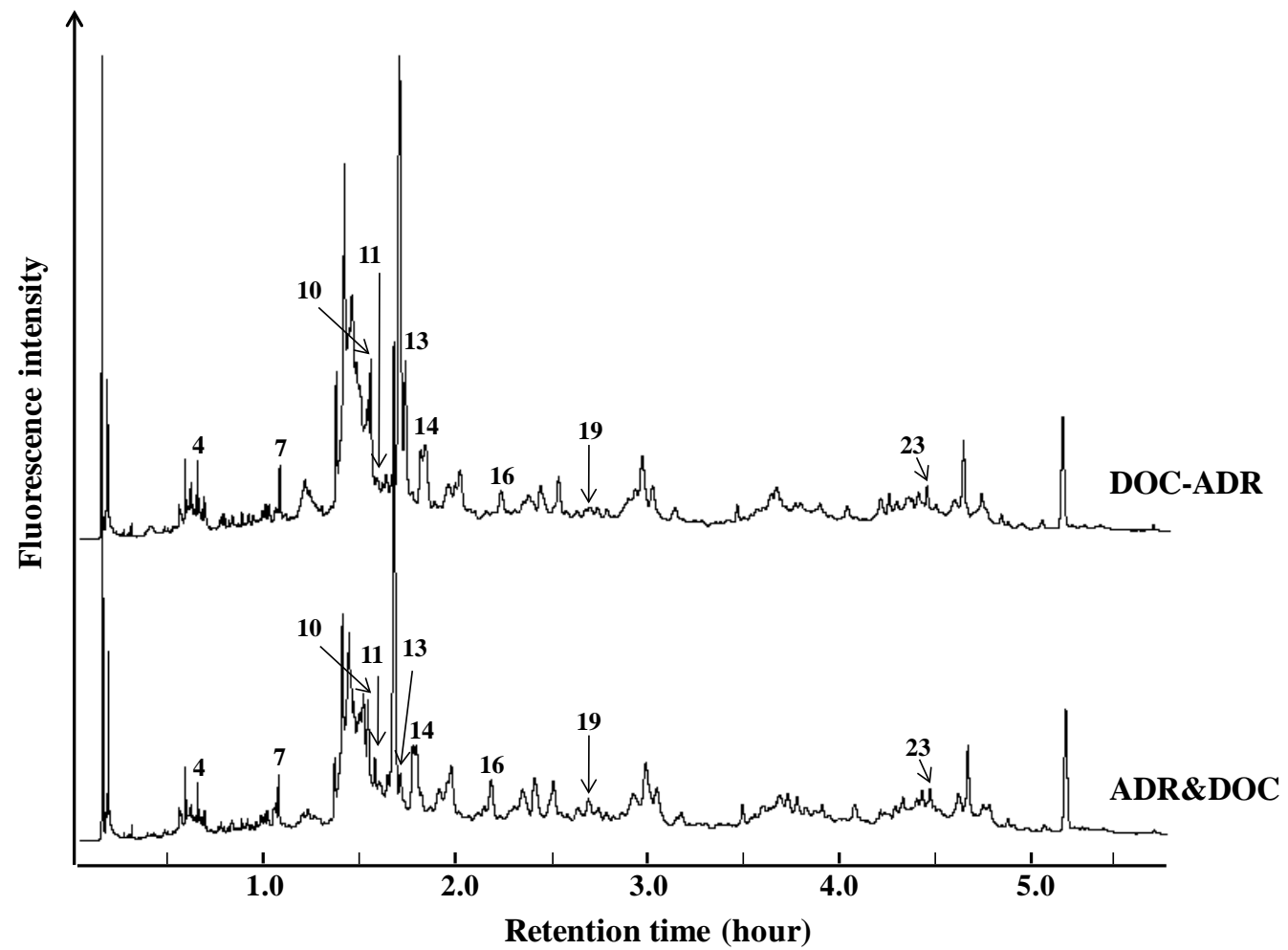


Fig. 3

Glycolytic pathway

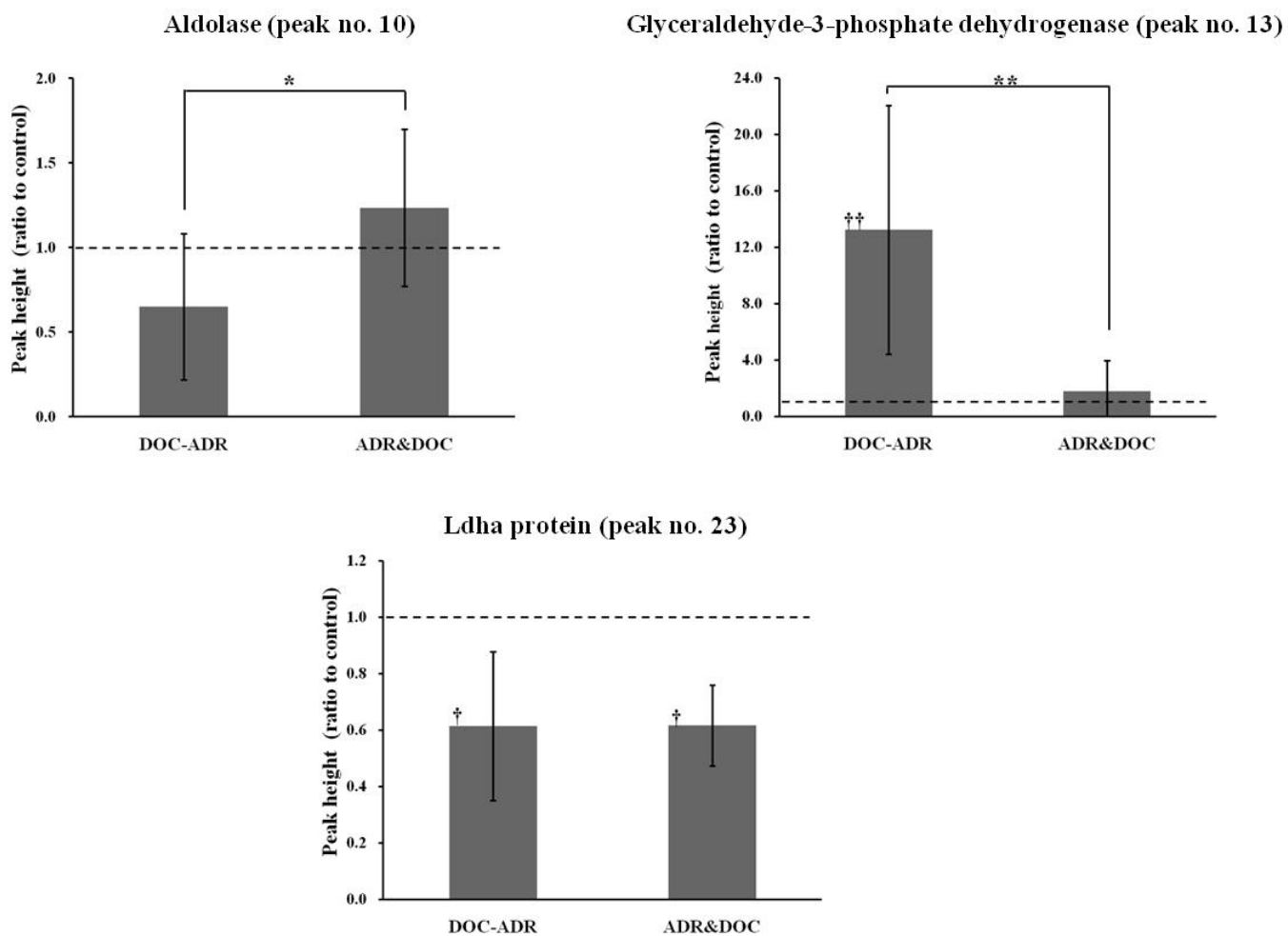
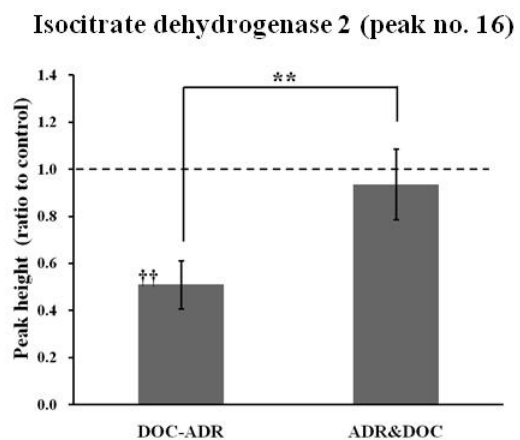
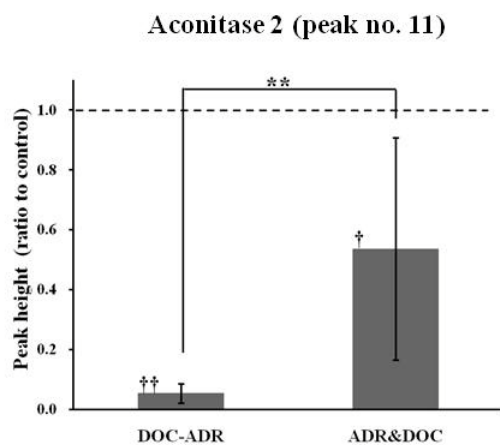


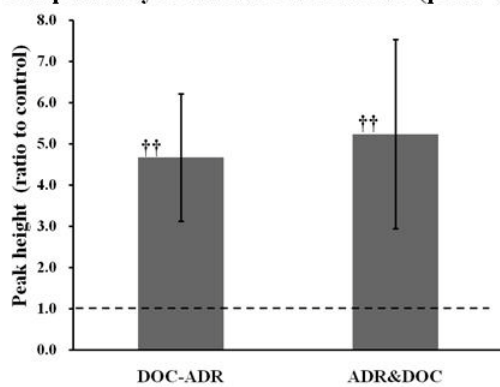
Fig. 3 (continued)

TCA cycle



Electron transport chain

Ubiquinol-cytochrome c reductase (peak no. 7)



Electron transferring flavoprotein (peak no. 19)

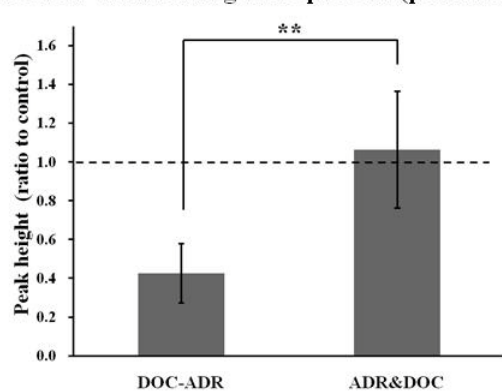
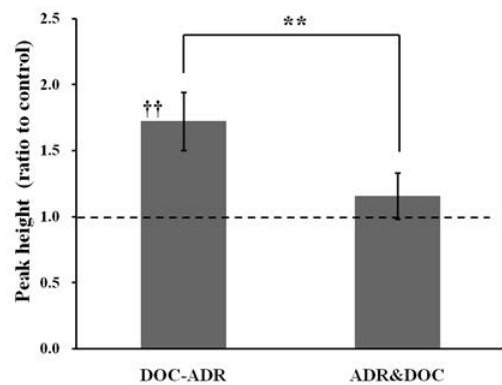


Fig. 3 (continued)

Other

Diazepam binding inhibitor (peak no. 4)



Creatine kinase (peak no. 14)

